Pure Appl. Chem., Vol. 82, No. 11, pp. 2167–2174, 2010.
doi:10.1351/PAC-CON-09-11-19

Nanocomposite polymer electrolytes prepared by in situ polymerization on the surface of nanoparticles for lithium-ion polymer batteries*

Ji Zhou, Deshu Gao‡, Zhaohui Li, Gangtie Lei, Tiepeng Zhao, and Xiaohua Yi

Key Laboratory of Environmentally Friendly Chemistry and Applications of Ministry of Education, College of Chemistry, Xiangtan University, Xiangtan, Hunan 411105, China

Abstract: A kind of nanocomposite polymer based on poly(acrylonitrile-methyl methacrylate) [P(AN-MMA)] copolymer was prepared by in situ polymerization of monomers on the surface of TiO_2 nanoparticles, which come from the hydrolysis of $Ti(OC_4H_9)_4$. Analysis of Fourier transform-infrared (FT-IR) spectra indicated that the acrylonitrile (AN) monomers copolymerized with the methyl methacrylate (MMA) monomers by breaking their own double bonds. The dependence of ionic conductivity on temperature for the resulting nanocomposite polymer electrolyte (NCPE) followed the Arrhenius equation. The ionic conductivity of the NCPE was 1.12×10^{-3} S cm^{-1} at room temperature when the nanocomposite polymer membrane (NPM) contained 10.8 % of mass fraction of TiO_2 nanoparticles.

Keywords: in situ polymerization; lithium-ion batteries; nanocomposite polymer electrolytes; P(AN-MMA); porous membranes.

INTRODUCTION

The development of portable electric devices, especially mobile phones and notebook computers, has led to a strong need for high energy density batteries in the last decade. Among various types of batteries, lithium-ion batteries are the most promising choice to meet this requirement. In order to enhance their energy density, lithium-ion batteries have been developed into a plastic-like power source system, called a polymeric lithium-ion battery (PLIB). In PLIBs, the nonaqueous electrolyte was gelled with polymer or absorbed in polymer matrix, leading to little of the free electrolyte within the battery container. Due to trapping of the electrolyte, PLIBs can use the polymeric container instead of the metal one, which is used in liquid-state lithium-ion batteries. As a result, the energy density of PLIBs enhances. In addition, PLIBs can be made into irregular shapes. It is well known that the ionic conductivity of polymer electrolytes is lower than that of liquid electrolytes on account of the high viscosity. Therefore, polymer electrolytes play a key role in influencing the electrochemical performances of PLIBs.

A few research works on polymer electrolytes have been done since Wright et al. found the conductivity of the polymer-salt system. Due to low conductivity of solid polymer electrolytes (SPEs),

---

*Paper based on a presentation at the 5th International Symposium on Novel Materials and Their Synthesis (NMS-V) and the 19th International Symposium on Fine Chemistry and Functional Polymers (FCFP-XIX), 18–22 October 2009, Shanghai, China. Other presentations are published in this issue, pp. 1975–2229.

‡Corresponding author: Tel.: +86 731 58293781; Fax: +86 731 58292477; E-mail: gaod@xtu.edu.cn

some molecular solvents like alkyl carbonates were added into the SPE, forming gelled polymer electrolyte (GPE). The GPE showed high ionic conductivity near to that of liquid electrolyte, but poor mechanical properties. The addition of nanoscale particles into the SPE, which forms a nanocomposite polymer electrolyte (NCPE), is another way to enhance the ionic conductivity as well as mechanical properties [1–4]. As a kind of solid plasticizer, the nanoparticles hinder the rearrangement of polymer chains, leading to a decrease in the crystallinity of polymer matrix. Moreover, they can weaken the interaction between the polar groups of polymer chains and lithium-ions by Lewis acid–base effect [5–9].

The GPE has poor mechanical properties, whereas the NCPE has low ionic conductivity. To merge high ionic conductivity and good mechanical properties, a kind of porous gelled polymer electrolyte (PGPE) based on the fluoride-containing polymers was found by A. S. Gozdz et al. [10]. The fabrication process of the PPGE includes mainly three steps: the first is to cast a polymer solution on the substrate, forming a self-supporting polymer membrane at high temperature; the second is to extract the plasticizer from the polymer membrane, forming a porous structure; the third is to immerse the porous polymer membrane in electrolyte, forming the PGPE. The first and second steps can be carried out in a normal environment while the third step must be performed under a moisture-free environment. In the PPGE, there are three phases: the polymer matrix, the gelled polymer matrix, and the absorbed electrolyte solution. The ions migrate in the electrolyte solution so the ionic conductivity of the PPGE closes to that of the electrolyte solution. The polymer-matrix-like backbone supports the PGPE to guarantee its mechanical properties.

Owing to the above-mentioned characteristics, a large number of works about the PGPE, which are based on poly(vinylidene fluoride) (PVDF) and its copolymers poly(vinylidene fluoride-*co*-hexafluoropropylene) (P(VDF-HFP)), have been reported [11–34]. Although the PVDF and P(VDF-HFP) are chemically and electrochemically stable in alkyl carbonate-based electrolyte, they are expensive materials compared with other polymers such as PAN, PMMA, polyvinyle chloride (PVC), poly(ethylene glycol) (PEG), and PEO. As PAN and PMMA are able to dissolve in the alkyl carbonates, which are usually used as the solvent of nonaqueous electrolyte for lithium-ion batteries, it is necessary to improve their chemical stability. Fortunately, the copolymerization of AN monomers with other monomers, for example, MMA, vinyl acetate (VAc), butyl acrylate (BA), etc., can improve the chemical stability of the resultant copolymers in carbonate-based electrolyte [35–46].

In this study, we prepare a kind of NCPE by in situ copolymerization of the AN monomers with MMA monomers on the surface of TiO_2 nanoparticles, which come from hydrolysis of $Ti(OC_4H_9)_4$. The resultant nanocomposites are characterized by Fourier transform-infrared (FT-IR) spectra and NMR spectrum, and show no dissolution in 1 M $LiPF_6$/ethyl carbonate (EC)/diethyl carbonate (DEC) (1:1, volume). The electrochemical properties of the obtained NCPE are investigated here.

EXPERIMENTAL

Synthesis and characterization of nanocomposite polymer

TiO_2 nanoparticles were firstly produced by hydrolysis in a certain amount of $Ti(OC_4H_9)_4$ in a solution of MMA and AN monomers (the volume of MMA and AN monomers was 2 and 8 ml, respectively). The reaction took place in a four-necked flask equipped with a nitrogen inlet, a reflux condenser, an addition funnel, and a mechanical stirrer. Subsequently, 0.0165 g sodium lauryl sulfate emulsifier was added dropwise slowly into the flask under vigorous agitation within 1 h. After that, 0.1850 g of potassium persulfate ($K_2S_2O_8$) initiator was added and agitated for 5 h at 60 °C. The formed precipitates were filtrated and washed with distilled water and ethanol to remove the impurities such as residual monomers and initiator. A white powder was finally obtained by drying the washed precipitates under vacuum at 80 °C for 24 h.

^1H NMR spectra of the powders (dissolve in dimethylsulfoxide-*d*6) were taken by a Bruker DRX-300 NMR spectrometer using tetramethylsilane as an internal standard reference. The IR spectra were recorded on Perkin-Elmer FTIR 1710 spectrometer covering a range of 450–4000 cm^{-1}. Solubility test was carried out by weighing the difference mass of the nanocomposite polymer powder before and after immersion in an electrolyte of 1 M $LiPF_6$/EC/DEC (volume 1:1) overnight.

Preparation of polymer membranes

0.5 g of the obtained polymer powders were dissolved in 5 ml *N*-methyl pyrrolidone (NMP), which contains 0.35 ml dibutyl phthalate (DBP), forming a viscous solution after agitation with an ultrasonic stirrer. The resulting solution was spread on a clean glass plate and then dried under vacuum at 80 °C for 8 h. After evaporation of NMP, the glass plate was cooled to room temperature. A polymer membrane was then peeled off from the glass plate and immersed in ether to extract the plasticizer DBP. At last, a nanocomposite polymer membrane (NPM) was produced after being dried at 50 °C under vacuum for 2 h.

Electrochemical measurement of NCPE

The NCPE was produced by immersing the NPM into 1 M solution of $LiPF_6$/EC/DEC (volume 1:1) for 2 h. After the excessive solution at the surface of the NCPE was removed with filler paper, the NCPE was sandwiched between two symmetrical stainless steel (SS) blocking electrodes. Using an EG&G Potentiostat/Golvannostat M273 electrochemical analysis system in conjunction with an M5210 Lock-in amplifier, the resistance of the NCPE was measured. The frequency ranged from 1 Hz to 100 kHz, and ac amplitude was 5 mV. The bulk resistance of NCPE was found from the impedance spectrum. Thus, the ionic conductivity was calculated based on the following equation:

$$\kappa = d/(S \times R_b) \tag{1}$$

where κ is the ionic conductivity, R_b the bulk resistance, d and S the thickness and area of the specimen, respectively.

RESULTS AND DISCUSSION

Figure 1 shows the ^1H NMR spectrum of the copolymer. The chemical shift at 1.17–1.40 ppm belongs to the methyl proton of the MMA unit. The methoxy proton of the MMA unit separately appeared at 3.55–3.69 ppm, whereas the peaks of methylene protons in MMA at 1.93–2.21 ppm were overlapped with the peaks of the methylene protons in AN. The peak of the protons of methine appears at 3.03–3.24 ppm.

Figure 2a shows the FTIR spectra of pure P(AN-MMA) membrane and TiO_2. The stretching vibration peak of the C≡N group appears at 2243 cm^{-1} for P(AN-MMA). The vibration peak at 1730 cm^{-1} is assigned to the C=O stretching of P(AN-MMA). The vibration peaks located at 2950 and 1384 cm^{-1} are ascribed to asymmetric stretching and symmetric bending vibrations of CH_3 group, respectively. The bending frequency at 1143 cm^{-1} corresponds to CH_2 groups. The vibration peak appearing at 1222 cm^{-1} is ascribed to the C–O bonds of P(AN-MMA) copolymer. The vibration peaks at 3457 and 1647 cm^{-1} can be assigned to the stretching and bending vibrations of OH groups for absorbed water. Vibration peaks between 1675 and 1640 cm^{-1} were not found, which belong to the characteristic vibration C=C bonds of olefin. As a result, it was deduced that the copolymerization of AN monomers with MMA monomers may be carried out by breaking their own double bonds. The absorption peak at 500 cm^{-1} is assigned to the characteristic vibration of TiO_2.

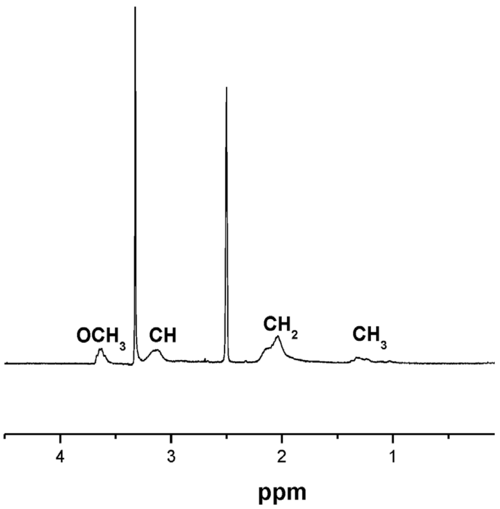

Fig. 1 ^{1}H NMR spectrum of the pure synthesized P(AN-MMA) copolymer. (Solvent: DMSO-d_6, reference: TMS).

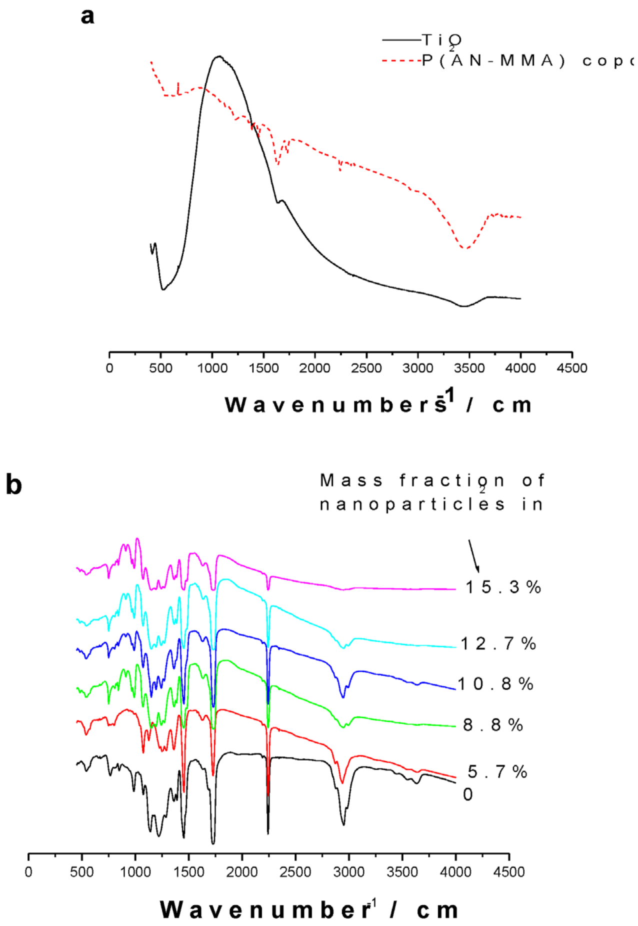

Fig. 2 FT-IR spectra of (a) pure P(AN-MMA) copolymer, and TiO$_2$; (b) NPMs containing various amounts of TiO$_2$ nanoparticles.

Figure 2b shows the FTIR spectra of the NPMs containing various amounts of TiO_2 nanoparticles. The vibration peaks at 3018 and 2980 cm^{-1}, which are assigned to nonsymmetrical and symmetrical stretching vibration of CH_2 groups, shifted to the lower frequencies of 2990 and 2935 cm^{-1} because of the interaction between –COO– and TiO_2. The vibration peak at 3400 cm^{-1} is ascribed to OH stretching vibrations, indicating that there is a hydrogen bond interaction between TiO_2 and polymer chains.

Solubility of the resulting nanocomposite polymer was summarized in Table 1. Although both the PAN and PMMA can fully dissolve in 1 M $LiPF_6$/EC/DEC (volume 1:1), their copolymer can dissolve only a little in the electrolyte. Due to interaction between nanoparticles and polymer chains, the obtained nanocomposite polymer cannot dissolve in the electrolyte.

Table 1 Ionic conductivity at room temperature and the calculated activation energy for ion transportation of the NCPEs containing various amounts of TiO_2 nanoparticles.

Mass fraction of TiO_2 in the NPMs wt %	Solubility of the NPMs in 1 M $LiPF_6$/EC/DEC	Ionic conductivity of the NCPE $\kappa/10^{-3}$ S cm^{-1}	Activation energy for ions transportation of the NCPE E_a/kJ mol^{-1}
0	Little solution	0.45	11.42
5.7	No solution	0.53	11.03
8.8	No solution	0.61	10.01
10.8	No solution	1.12	6.77
12.7	No solution	0.76	7.97
15.3	No solution	0.58	10.72

Figure 3 shows the AC impedance spectra of the NCPEs containing different amounts of TiO_2. The intercept on the Z_{re} axis corresponding to the left terminal of semicircles represents the bulk resistance (R_b) of polymer electrolyte. The ionic conductivity of the NCPE was calculated from eq. 1 and listed in Table 1. It increases with the increasing amount of TiO_2 nanoparticles in the NCPE when the mass fraction is not more than 10.8 %. The NCPE without TiO_2 nanoparticles had the lowest conduc-

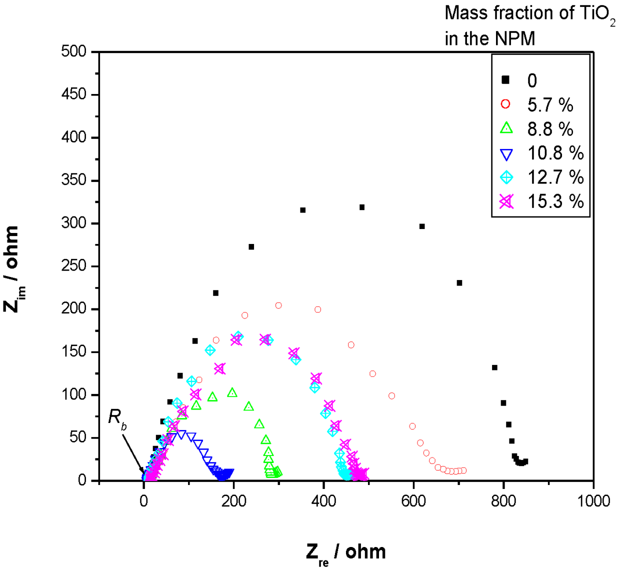

Fig. 3 AC impedance spectra of the NCPEs containing various amounts of TiO_2 nanoparticles at room temperature.

tivity of 0.45 × 10^{-3} S cm^{-1} at room temperature. At the amount of 10.8 wt %, the NCPE achieved the highest ionic conductivity, 1.12 × 10^{-3} S cm^{-1}.

On one hand, the volume of the interfacial layers between polymer matrix and TiO_2 nanoparticles increases with the amount of TiO_2 nanoparticles in the polymer membrane. On the other hand, the competition between TiO_2 and polar groups such as C≡N and C=O with respect to lithium ions facilitates their migration. In this case, the ionic conductivity of the NCPE increases with the addition of TiO_2 nanoparticles. On the contrary, excessive TiO_2 nanoparticles aggregate easily in the polymer matrix due to their high surface energy. As a result, the volume of the interfacial layers decreases and the effective number of the OH groups, which compete for lithium ions with C≡N and C=O units, on the surface of nanoparticles reduces. Therefore, the ionic conductivity of polymer electrolyte decreases with further addition of TiO_2 nanoparticles.

Figure 4 exhibits the dependence of ionic conductivity on temperature ranged from 25 to 80 °C for the NCPE. These curves appears linear so the activation energy for ions transportation, E_a, can be calculated from the Arrhenius equation, $\kappa = \kappa_0 \exp(-E_a/RT)$, where R is the gas content, κ_0 the pre-exponential index, and T the test absolute temperature, respectively. The calculated values of activation energy for ion transportation are summarized in Table 1. The activation energy for ion transportation was found to have reached the minimum value, namely, 6.77 kJ mol^{-1} when the NCPE contained 10.8 wt % TiO_2 nanoparticles.

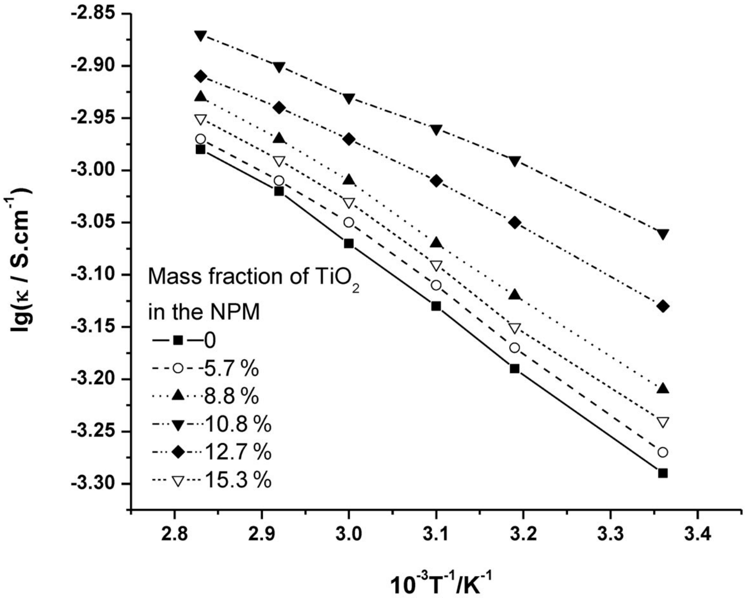

Fig. 4 Log κ-T^{-1} curve of the NCPEs containing various amounts of TiO_2 nanoparticles ranged from 20 to 80 °C.

CONCLUSION

The NCPEs based on P(AN–MMA) copolymer have been successfully prepared by in situ copolymerization of AN monomers with MMA monomers on the surface of TiO_2 nanoparticles. The polymer membranes from the nanocomposites are chemically stable in 1 M $LiPF_6$/EC/DEC (volume 1:1) electrolyte for a long time. The copolymerization reaction of AN monomers with MMA monomers is suggested to be carried out by breaking their own C=C bonds. The optimal mass fraction of TiO_2 nanoparticles in polymer matrix is 10.8 %. At this amount, the NCPE had a high ionic conductivity of 1.12×10^{-3} S cm^{-1} at room temperature and a low activation energy for ion transportation, 6.77 kJ mol^{-1}. The results suggest its application in PLIBs.

ACKNOWLEDGMENTS

Support from the Natural Science Foundation of Hunan Province (09JJ5008), the Open Fund from State Key Laboratory of Chemical Engineering in East China University of Science and Technology (SKL-ChE-08C06), and the Doctoral Starting Fund from Xiangtan University (05QDZ18) is greatly appreciated.

REFERENCES

1. F. Croce, G. B. Appetecchi, L. Persi, B. Scrosati. *Nature* **394**, 456 (1998).
2. F. Croce, R. Curini, A. Martinelli, L. Persi, F. Ronci, B. Scrosati, R. Caminiti. *J. Phys. Chem. B* **103**, 10632 (1999).
3. G. B. Appetecchi, F. Croce, L. Persi, F. Ronci, B. Scrosati. *Electrochim. Acta* **45**, 1481 (2000).
4. B. Scrosati, F. Croce, L. Persi. *J. Electrochem. Soc.* **147**, 1718 (2000).
5. R. Y. Hong, L. L. Chen, J. H. Li, H. Z. Li, Y. Zheng, J. Ding. *Polym. Adv. Technol.* **18**, 901 (2007).
6. C. G. Chen, D. Yebassa, D. Raghavan. *Polym. Adv. Technol.* **18**, 574 (2007).
7. F. Croce, L. Persi, B. Scrosati, F. Serraino-Fiory, E. Plichta, M. A. Hendrickson. *Electrochim. Acta* **46**, 2457 (2001).
8. W. Wieczorek, P. Lipka, G. Zukowska, H. Wycislik. *J. Phys. Chem. B* **102**, 6968 (1998).
9. P. P. Prosini, P. Villano, M. Carewska. *Electrochim. Acta* **48**, 227 (2002).
10. A. S. Gozdz, C. N. Schmutz, J. M. Tarascon. U.S. Patent 5,296,138 (1994).
11. H. Huang, S. Lowunder. *J. Eletrochem. Soc.* **148**, A279 (2001).
12. A. Magistris, P. Mustarelli, E. Quastarone, P. Piaggio, A. Bottino. *Electrochim. Acta* **46**, 1635 (2001).
13. D. W. Kim, K. A. Noh, J. H. Chan, S. H. Kim, J. M. Ko. *Solid State Ionics* **144**, 329 (2001).
14. Y. J. Wang, D. Kim. *Electrochim. Acta* **52**, 3181 (2007).
15. Z. H. Li, P. Zhang, H. P. Zhang, Y. P. Wu, X. D. Zhou. *Electrochem. Commun.* **10**, 791 (2008).
16. Z. H. Li, C. Cheng, X. Y. Zhan, Y. P. Wu, X. D. Zhou. *Electrochim. Acta* **54**, 4403 (2009).
17. A. M. Stephan, D. Teeters. *J. Power Sources* **119–121**, 460 (2003).
18. H. P. Zhang, P. Zhang, Z. H. Li, M. Sun, Y. P. Wu, H. Q. Wu. *Electrochem. Commun.* **9**, 1700 (2007).
19. G. C. Li, Z. H. Li, P. Zhang, H. P. Zhang, Y. P. Wu. *Pure Appl. Chem.* **80**, 2553 (2008).
20. Z. H. Li, G. Y. Su, X. Y. Wang, D. S. Gao. *Solid State Ionics* **176**, 1903 (2005).
21. Z. H. Li, P. Zhang, H. P. Zhang, Y. P. Wu, X. D. Zhou. *Electrochem. Commun.* **10**, 791 (2008).
22. Z. H. Li, H. P. Zhang, P. Zhang, Y. P. Wu, X. D. Zhou. *J. Power Sources* **184**, 562 (2008).
23. P. Zhang, G. C. Li, H. P. Zhang, L. C. Yang, Y. P. Wu. *Electrochem. Commun.* **11**, 161 (2009).
24. H. P. Zhang, P. Zhang, G. C. Li, Y. P. Wu, D. L. Sun. *J. Power Sources* **189**, 594 (2009).
25. Q. Z. Xiao, X. Z. Wang, W. Li, Z. H. Li, T. J. Zhang, H. L. Zhang. *J. Membr. Sci.* **334**, 117 (2009).
26. M. Stolarska, L. Niedzicki, R. Borkowska, A. Zalewska, W. Wieczorek. *Electrochim. Acta* **53**, 1512 (2007).
27. Y. J. Wang, D. Kim. *J. Power Sources* **166**, 202 (2007).
28. A. Manuel Stephan, K. S. Nahm, T. P. Kumar, M. A. Kulandainathan, G. Ravi, J. Wilson. *J. Power Sources* **159**, 1316 (2006).
29. G. C. Li, P. Zhang, H. P. Zhang, L .C. Yang, Y. P. Wu. *Electrochem. Commun.* **10**, 1883 (2008).
30. P. Zhang, G. C. Li, H. P. Zhang, L. C. Yang, Y. P. Wu. *Electrochem. Commun.* **11**, 161 (2009).
31. H. P. Zhang, P. Zhang, G. C. Li, Y. P. Wu, D. L. Sun. *J. Power Sources* **189**, 594 (2009).

32. S. Ferrari, E. Quartarone, P. Mustarelli, A. Magistris, M. Fagnoni, S. Protti, C. Gerbaldi, A. Spinella. *J. Power Sources* **195**, 559 (2010).
33. J. M. Song, H. R. Kang, S. W. Kim, W. M. Lee, H. T. Kim. *Electrochim. Acta* **48**, 1339 (2003).
34. P. Mustarelli, E. Quartarone, C. Capiglia, C. Tomasi, A. Magistris. *Solid State Ionics* **122**, 285 (1999).
35. Y. H. Liao, D. Y. Zhou, M. M. Rao, W. S. Li, Z. P. Cai, Y. Liang, C. L. Tan. *J. Power Sources* **189**, 139 (2009).
36. F. Yuan, H. Z. Chen, H. Y. Yang, H. Y. Li, M. Wang. *Mater. Chem. Phys.* **89**, 390 (2005).
37. J. D. Jeon, B. W. Cho, S. Y. Kwak. *J. Power Sources* **143**, 219 (2005).
38. H. Cheng, C. B. Zhu, B. Huang, M. Lu, Y. Yang. *Electrochim. Acta* **52**, 5789 (2007).
39. S. Rajendran, M. R. Prabhu, M. U. Rani. *J. Power Sources* **180**, 880 (2008).
40. S. S. Zhang, M. H. Ervin, K. Xu, T. R. Jow. *Electrochim. Acta* **49**, 3339 (2004).
41. W. H. Pu, X. M. He, L. Wang, Z. Tian, C. Y. Jiang, C. R. Wan. *J. Membr. Sci.* **280**, 6 (2006).
42. P. Zhang, H. P. Zhang, G. C. Li, Z. H. Li, Y. P. Wu. *Electrochem. Commun.* **10**, 1052 (2008).
43. D. Y. Zhou, G. Z. Wang, W. S. Li, G. L. Li, C. L. Tan, M. M. Rao, Y. H. Liao. *J. Power Sources* **184**, 477 (2008).
44. S. Shi, S. Kuroda, K. Hosoi, H. Kubota. *Polymer* **46**, 3567 (2005).
45. R. Baskaran, S. Selvasekarapandian, N. Kuwata, J. Kawamura, T. Hattori. *Solid State Ionics* **177**, 2679 (2006).
46. Z. Tian, X. M. He, W. H. Pu, C. R. Wan, C. Y. Jiang. *Electrochim. Acta* **52**, 688 (2006).